

Microenvironmental Analysis of Biofilms

Part I - Microsensors

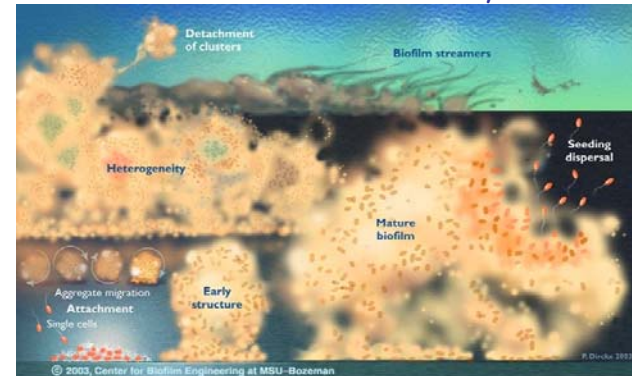
Michael Kühl

Marine Biological Laboratory
Department of Biology
University of Copenhagen

mkuhl@bio.ku.dk

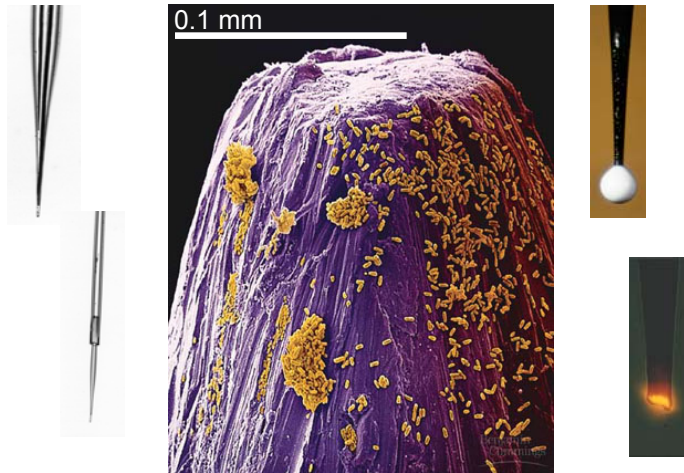
www.mbl.ku.dk/mkuhl

A biofilm is...a surface associated microbial community



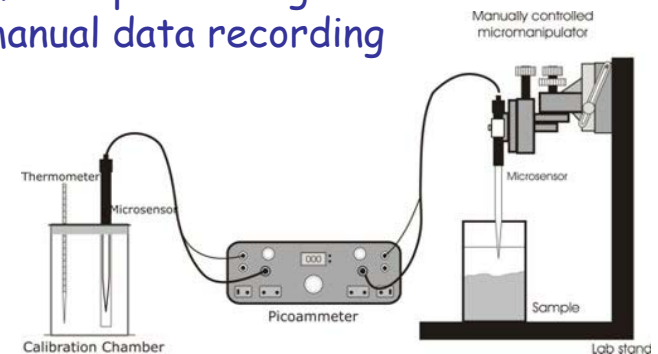
Microbial biofilms are a natural phenomenon that occurs in almost all environments. They are communities of microorganisms that are attached to a surface and encased in a self-produced extracellular matrix. Biofilms can form on a wide variety of surfaces, including natural and artificial materials. They are highly resistant to environmental stresses, including antibiotics, and can play a role in various biological processes, including disease and bioremediation. Biofilms are also a major concern in the food industry, as they can cause contamination and spoilage. Understanding the formation and structure of biofilms is essential for developing strategies to control and prevent their growth.

Measuring microbial activity at the appropriate scale ?



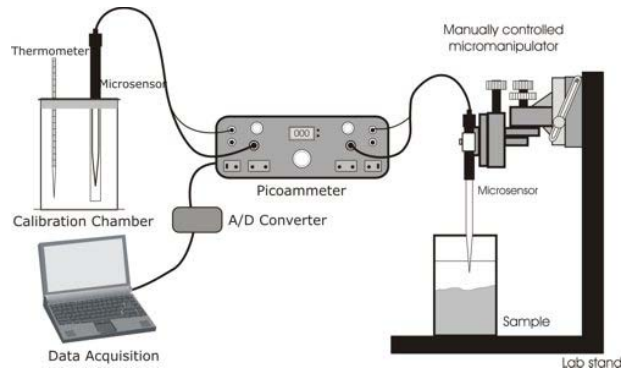
Simplest setup

- manual positioning
- manual data recording



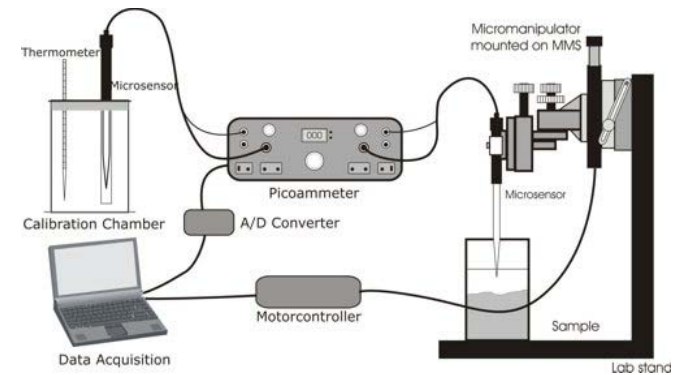
More fancy setup

- manual positioning
- automated data recording



Real fancy setup

- automatic positioning & data recording



Microsensors

Electrochemical

- **Potentiometric** sensors for:
pH, CO_2 , S^{2-} (solid state)
pH, CO_3^{2-} , NO_2^- , NO_3^- , NH_4^+ ,
 Ca^{2+} (LIX-based)
- **Amperometric** sensors for:
 O_2 , H_2S , N_2O , NO , H_2 , H_2O_2
flow, diffusivity
- **Voltammetric** sensors for:
Reduced Fe & Mn, O_2 , S_{tot} , ...
- **Microbiosensors** for:
 $\text{NO}_3^-/\text{NO}_2^-$, CH_4 , Glucose,
BOD, VFA
- **Diffusivity** sensors



Kühl & Revsbech 2001, Revsbech 2005, Kühl 2005

Potentiometric microsensors - pH

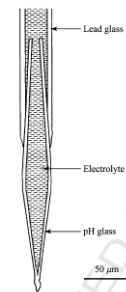


FIG. 2. Tip of glass pH microsensor. The cone made from pH-sensitive (i.e., hydrogen ion exchange) glass will integrate ambient pH over the entire length.

Integrated response over the exposed surface of the pH sensitive glass.

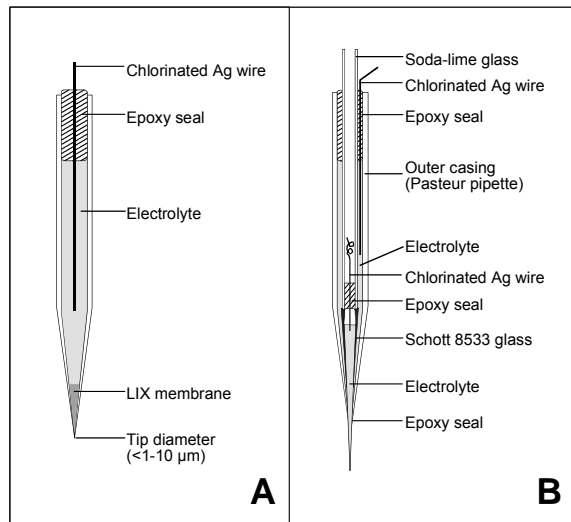
Fragile.

Potentiometric microsensors measure a Log-linear response of signal (mV) vs. Activity of ion.

At low ionic strength activity=concentration, but at higher ionic strength?

Revsbech 2005

Potentiometric microsenors - LIX



H^+
 Ca^{2+}
 NH_4^+

NO_2^-
 NO_3^{2-}
 CO_3^{2-}

PO_4^{3-}
 SO_4^{2-}

Short life

Drifting signal

Interferences

Kühl & Revsbech 2001

Microsenors

Electrochemical

- **Potentiometric** sensors for:
pH, CO_2 , S^{2-} (solid state)
pH, CO_3^{2-} , NO_2^- , NO_3^- , NH_4^+ ,
 Ca^{2+} (LIX-based)
- **Amperometric** sensors for:
 O_2 , H_2S , N_2O , NO , H_2 , H_2O_2
flow, diffusivity
- **Voltammetric** sensors for:
Reduced Fe & Mn, O_2 , S_{tot} , ...
- **Microbiosensors** for:
 NO_3^-/NO_2^- , CH_4 , Glucose,
BOD, VFA
- **Diffusivity** sensors



Kühl & Revsbech 2001, Revsbech 2005, Kühl 2005

Amperometric Clark-type O_2 microsenor

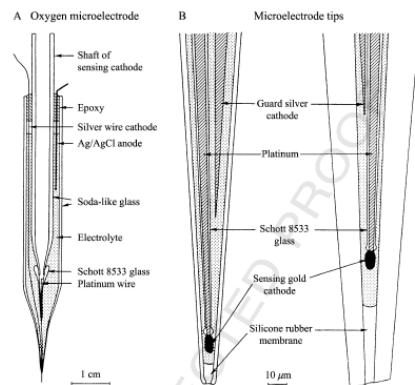


FIG. 1. Oxygen microsenor of the micro-Clark type shown with both a thin tip, which can be used for analysis where minimum sample disturbance is essential, and a sturdy tip for use in media that might otherwise cause sensor damage. The internal guard cathode removes oxygen from the internal electrolyte that might otherwise interfere. From Revsbech (1989), with permission from Limnology and Oceanography.

"Ideal" sensor

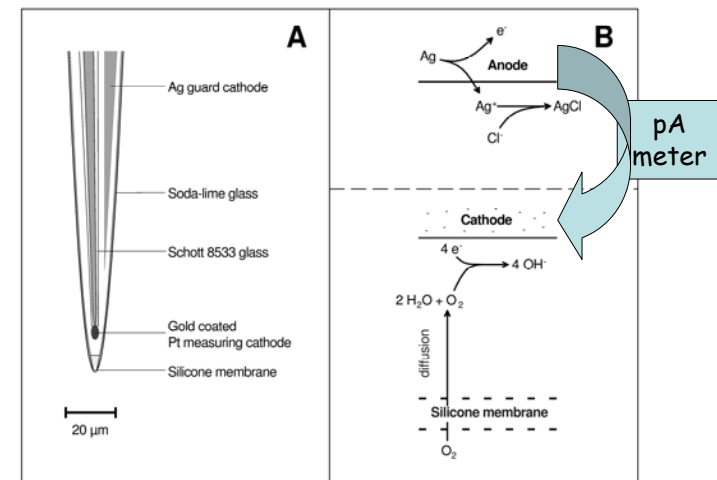
Low O_2 consumption
/Low stirring artefact

Linear, stable and fast response
(down to <0.2 s)

Taylorized performance
by varying tip dimensions

Revsbech 2005

Clark-type O_2 microsenor



Kühl & Revsbech 2001

Microsensors

Electrochemical

- **Potentiometric** sensors for:
pH, CO_2 , S^{2-} (solid state)
pH, CO_3^{2-} , NO_2^- , NO_3^- , NH_4^+ ,
 Ca^{2+} (LIX-based)
- **Amperometric** sensors for:
 O_2 , H_2S , N_2O , NO , H_2 , H_2O_2
flow, diffusivity
- **Voltammetric** sensors for:
Reduced Fe & Mn, O_2 , S_{tot} ,...
- **Microbiosensors** for:
 $\text{NO}_3^-/\text{NO}_2^-$, CH_4 , Glucose,
BOD, VFA
- **Diffusivity** sensors



Kühl & Revsbech 2001, Revsbech 2005, Kühl 2005

Nitrate/Nitrite micro-biosensor

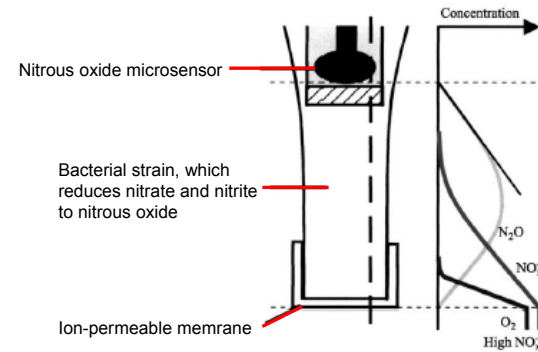


FIG. 6. Microscale biosensor for NO_3^- or NO_2^- . Bacteria in the tip convert incoming NO_3^- or nitrite plus nitrate (NO_2^-) to N_2O , which is subsequently monitored by the internal N_2O microsensor.

Microengineering using knowledge of diffusion, reaction kinetics and microbiology

Revsbech 2005

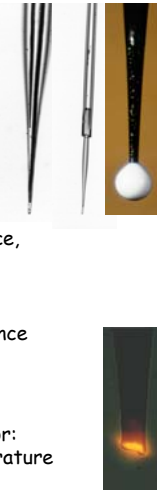
Microsensors

Electrochemical

- **Amperometric** sensors for:
 O_2 , H_2S , N_2O , NO , H_2 , H_2O_2
flow, diffusivity
- **Potentiometric** sensors for:
pH, CO_2 , S^{2-} (solid state)
pH, CO_3^{2-} , NO_2^- , NO_3^- , NH_4^+ ,
 Ca^{2+} (LIX-based)
- **Voltammetric** sensors for:
Reduced Fe & Mn, O_2 , S_{tot} ,...
- **Microbiosensors** for:
 $\text{NO}_3^-/\text{NO}_2^-$, CH_4 , Glucose,
BOD, VFA

Fiber-optic

- **Microprobes** for:
- radiance, irradiance,
scalar irradiance
(UV-NIR light)
- Surface detection
- Pigment fluorescence
- Diffusivity/Flow
- **Micro-opt(r)odes** for:
 O_2 , pH, CO_2 , temperature



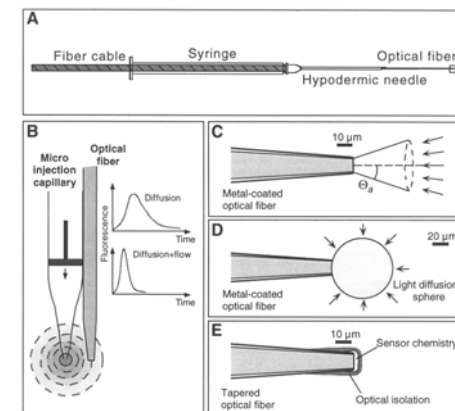
Kühl & Revsbech 2001, Revsbech 2005, Kühl 2005

Fiber-optic Microsensors

- Microprobes (A-D) for:**
- radiance, irradiance,
scalar irradiance (UV-
NIR light)
 - Surface detection
 - Pigment fluorescence
 - Diffusivity/Flow

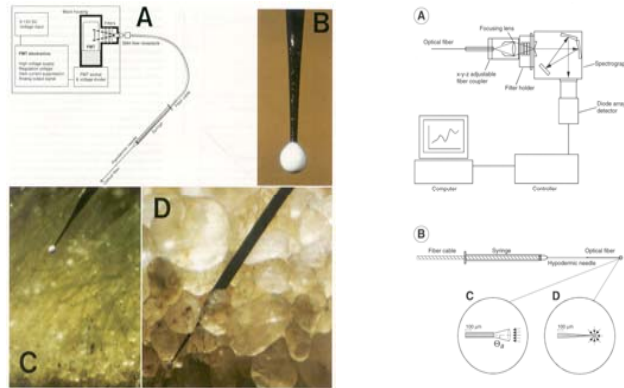
- Micro-opt(r)odes (E) for:**
- O_2 , pH, CO_2 ,
temperature

All based on multimode
graded index optical fibers
100/140 μm core/cladding
N.A. = 0.22



Kühl & Revsbech 2001

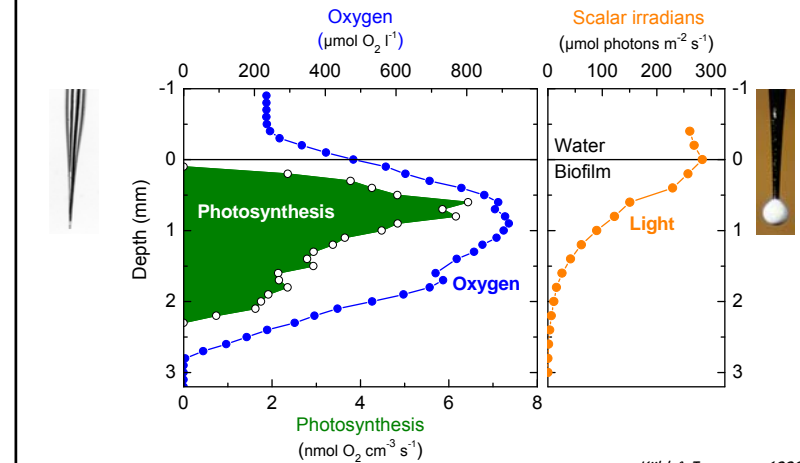
Microscale light measurements



Kühl et al. 1997

Kühl & Jørgensen 1992

Light and Photosynthesis



Kühl & Jørgensen 1992

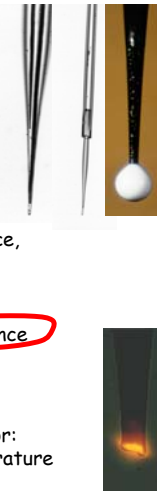
Microsensors

Electrochemical

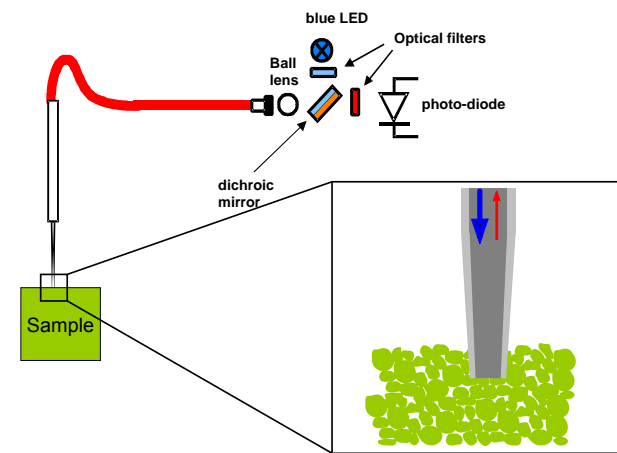
- **Amperometric** sensors for: O_2 , H_2S , N_2O , NO , H_2 , H_2O_2 flow, diffusivity
- **Potentiometric** sensors for: pH, CO_2 , S^{2-} (solid state) pH, CO_3^{2-} , NO_2^- , NO_3^- , NH_4^+ , Ca^{2+} (LIX-based)
- **Voltammetric** sensors for: Reduced Fe & Mn, O_2 , S_{tot} , ...
- **Microbiosensors** for: $\text{NO}_3^-/\text{NO}_2^-$, CH_4 , Glucose, BOD, VFA

Fiber-optic

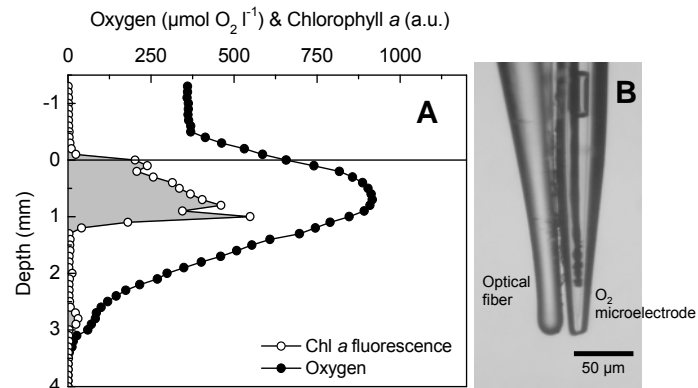
- **Microprobes** for:
 - radiance, irradiance, scalar irradiance (UV-NIR light)
 - Surface detection
 - Pigment fluorescence
 - Diffusivity/Flow
- **Micro-opt(r)odes** for: O_2 , pH, CO_2 , temperature



Microscale fluorescence measurements



Combined oxygen and fluorescence analysis



Kühl 2005

Fiber-optic Microsensors

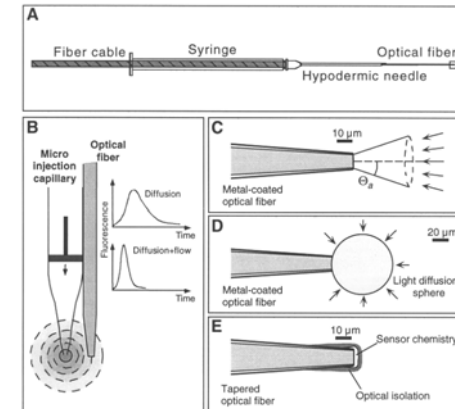
Microprobes (A-D) for:

- radiance, irradiance, scalar irradiance (UV-NIR light)
- Surface detection
- Pigment fluorescence
- Diffusivity/Flow

Micro-opt(r)odes (E) for:

- O_2 , pH, CO_2 , temperature

All based on multimode graded index optical fibers
100/140 μm core/cladding
N.A. = 0.22



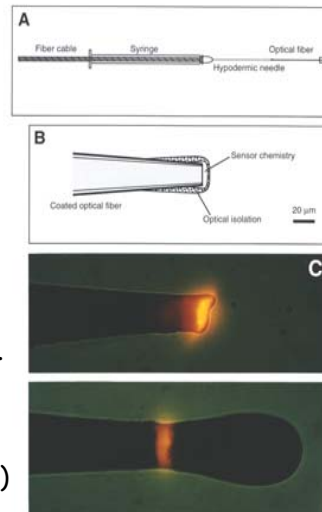
Kühl & Revsbech 2001

Micro-Optodes

Analyte dependend change in optical properties of an immobilized indicator dye.

Mostly based on dyes changing absorbance or luminescence.

Immobilization in various polymers (PVC, polystyrene, sol-gel.....)



Klimant et al. 1995

Optical oxygen measurement

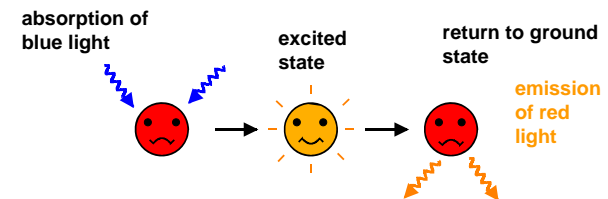
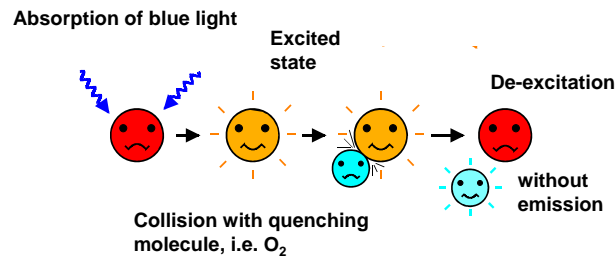


Photo-Luminescence of Ruthenium dyes & Platinum or Palladium porphyrins

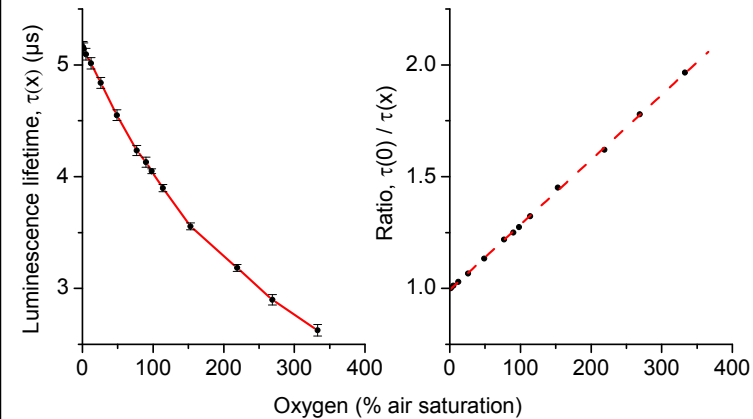
Optical oxygen measurement

Indicator luminescence is dynamically quenched by O_2



Ideal Stern-Volmer quenching response

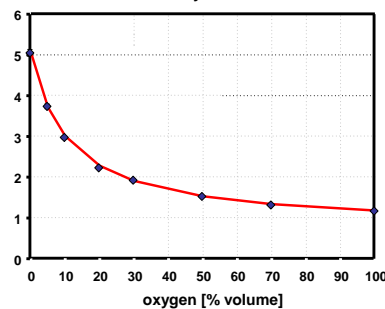
$$\frac{I_0}{I(x)} = \frac{\tau_0}{\tau(x)} = 1 + K_{SV} \cdot [O_2]_x$$



Kühl et al. 2007

Calibration

Luminescence intensity or lifetime



Modified version of the Stern-Volmer equation:

$$\frac{I}{I_0} = \frac{\tau}{\tau_0} = \frac{1-\alpha}{(1+K_{SV} \cdot [O_2])} + \alpha$$

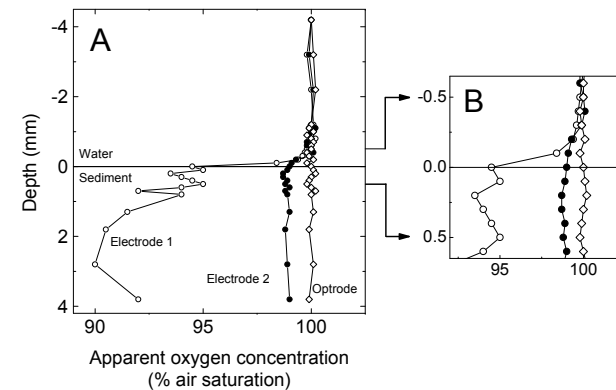
$$c = \frac{(I_0 - I)}{K_{SV} \cdot (I - I_0 \alpha)} = \frac{(\tau_0 - \tau)}{K_{SV} \cdot (\tau - \tau_0 \alpha)}$$

$$K_{SV} = \frac{I_0(c_2 - c_1) - (I_1 c_2 - I_2 c_1)}{(I_1 - I_2) \cdot c_1 \cdot c_2}$$

$$\alpha = \frac{I_1(1 + K_{SV} c_1) - I_0}{I_0 \cdot K_{SV} \cdot c_1}$$

Kühl 2005

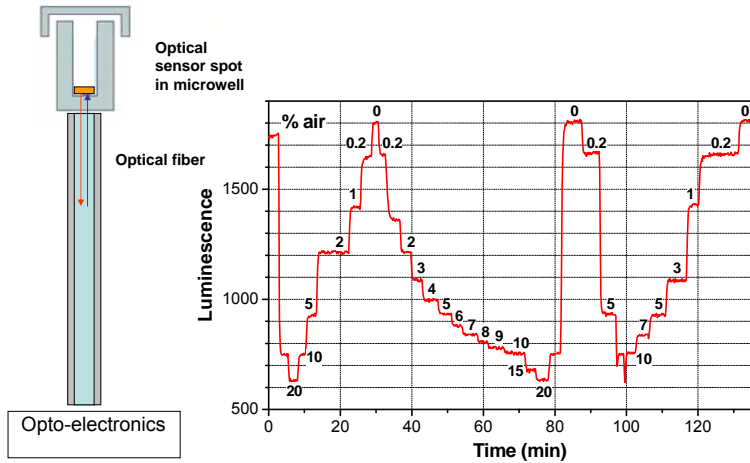
Oxygen optodes do not consume O_2



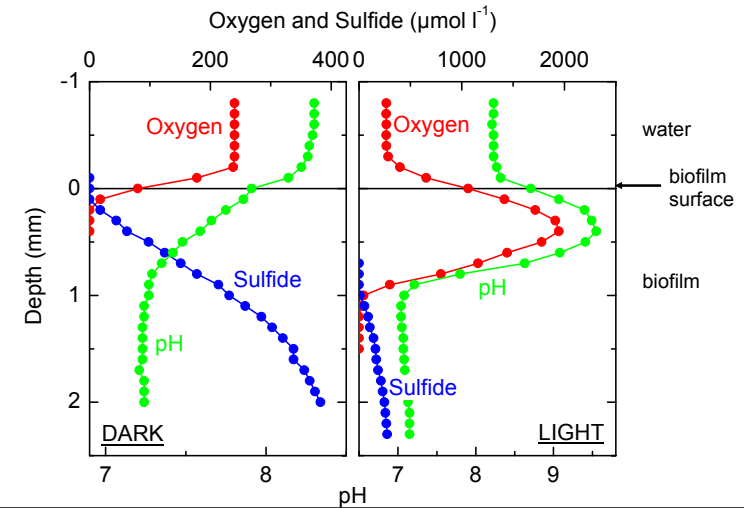
- And are not sensitive to sulfide ☹

Klimant, Mayer & Kühl 1995

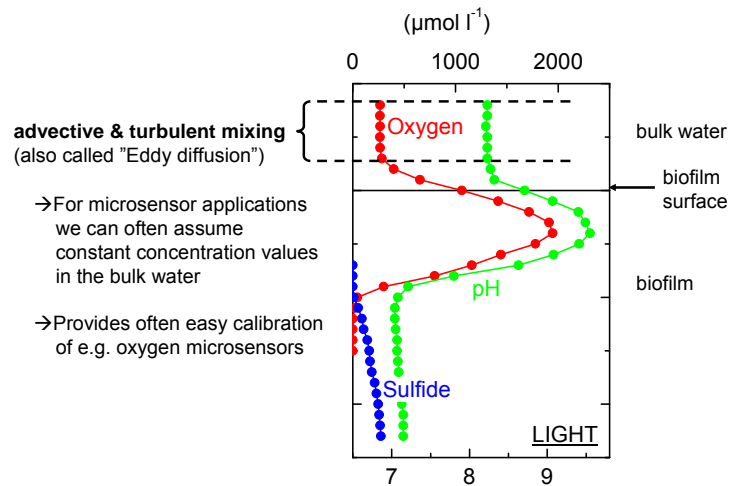
Fiber-based (or plate reader based) respirometry in microtiter wells (Silicone + Pt-porphyrin)



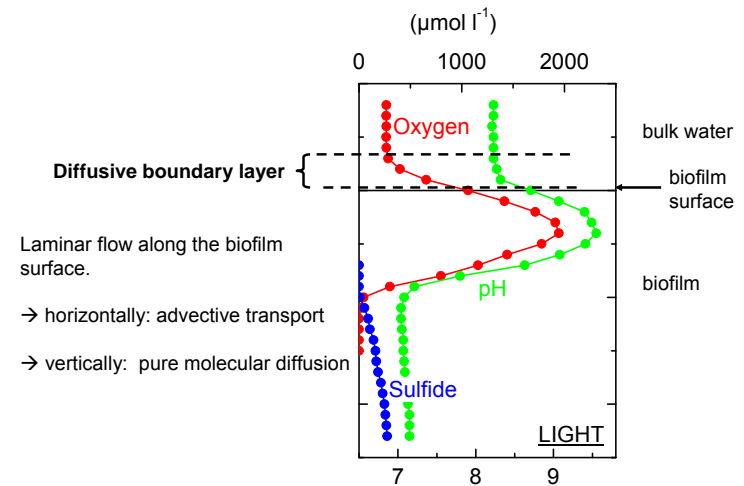
How to read concentration profiles?



1. Bulk water



2. Diffusive boundary layer (DBL)



The DIFFUSIVE BOUNDARY LAYER (DBL)

Exchange of solutes between water and sediment is due to a combination of turbulent transport (**eddy diffusion**, E) and **molecular diffusion**, D:

$$D_{\text{tot}} = E + D$$

In turbulent water $E \gg D$.
Turbulences are dampened close to structures until $E < D$.

In a 0.1-1 mm thin water layer (DBL) just above the structure, solute transport becomes dominated by molecular diffusion.

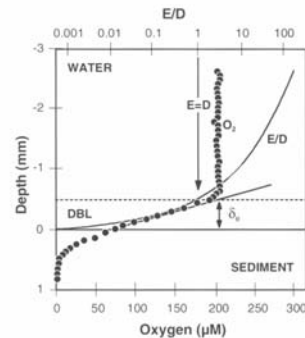
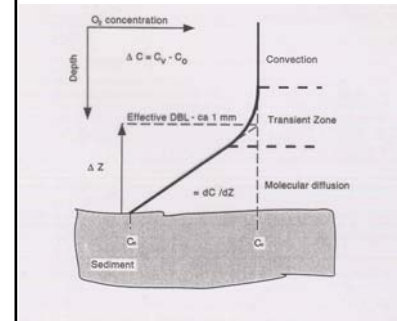
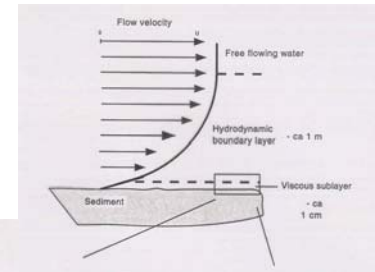


Fig. 5.5 Oxygen microgradient (n) at the sediment-water interface compared to the ratio, E/D (logarithmic scale), between the vertical eddy diffusion coefficient, E, and the molecular diffusion coefficient, D. Oxygen concentration was constant in the overflowing seawater. It decreased linearly within the diffusive boundary layer (DBL), and penetrated only 0.7 mm into the sediment. The DBL had a thickness of 0.45 mm. Its effective thickness, δ_b , is defined by the intersection between the linear DBL gradient and the constant bulk water concentration. The diffusive boundary layer occurs where E becomes smaller than D, i.e. where $E/D \approx 1$ (arrow). Data from Aarhus Bay, Denmark, at 15 m water depth during fall 1990 (Gundersen et al. 1995).

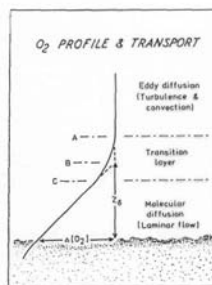
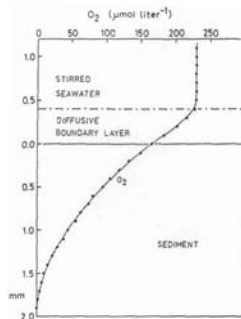
Diffusive boundary layers surround all surfaces and often limit mass transfer.



$$J = D_0 \frac{dC}{dz}$$

$$J = \frac{D_0}{\Delta z} (C_v - C_0) = k(C_v - C_0)$$

The DBL as a barrier towards solute exchange ?

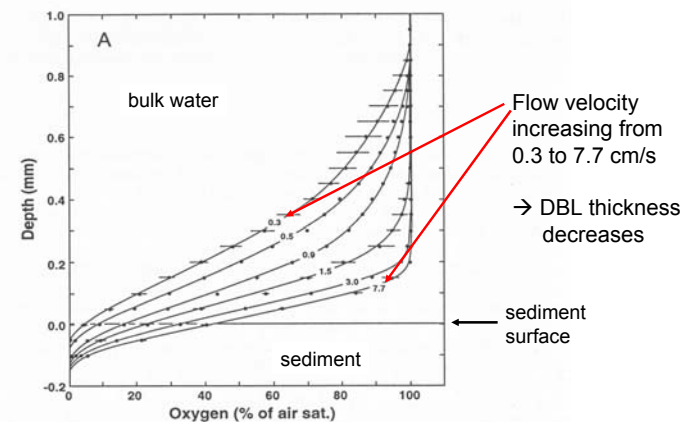


$$t \sim \frac{L^2}{2D_0}$$

Distance - diffusion time O_2

1 μm	- 0.3 msec
100 μm	- 3.0 sec
1 mm	- 4.0 min
1 cm	- 7.0 h
10 cm	- 25.0 d

The flow velocity of the bulk water determines the thickness of the DBL



Jørgensen (2001)

Simple Oxygen Profile Analysis

Fick's 1'st law:

$$J(x) = -\phi D(x) \frac{dC(x)}{dx}$$

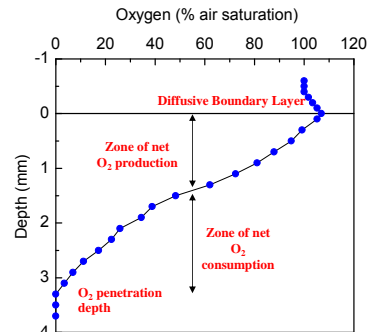


→ *netto*_production

Profile concave from left,

$$\frac{d^2C(x)}{dx^2} > 0 \Rightarrow R(x) - P(x) > 0$$

⇒ *netto*_consumption

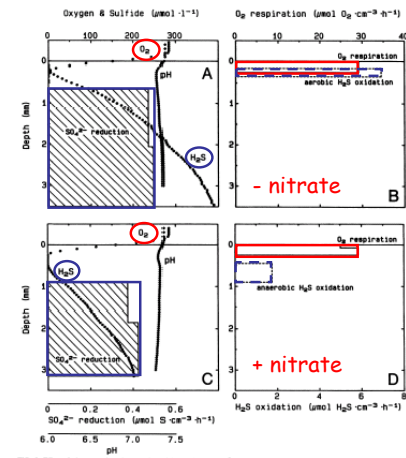


Profile straight line,

$$\frac{d^2C(x)}{dx^2} = 0 \Rightarrow R(x) - P(x) = 0$$

⇒ *pure*_diffusion

Sulfur cycling in a biofilm



Fick's 2nd law:

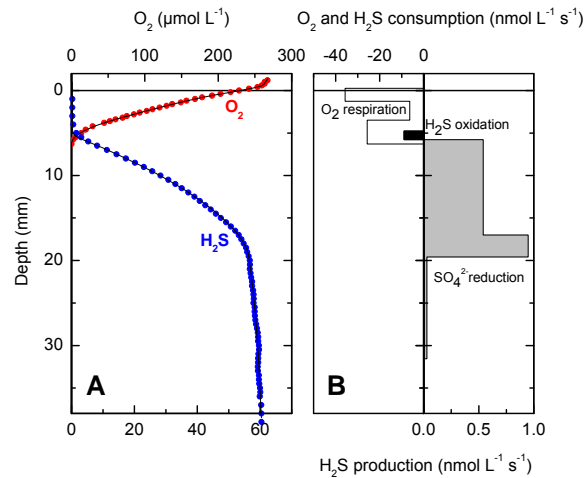
$$\frac{dC(x,t)}{dt} = D(x) \frac{d^2C(x,t)}{dx^2} - R(x,t) + P(x,t)$$

At steady-state $dC/dt=0$ causing:

$$P(x) - R(x) = -D(x) \frac{d^2C(x)}{dx^2}$$

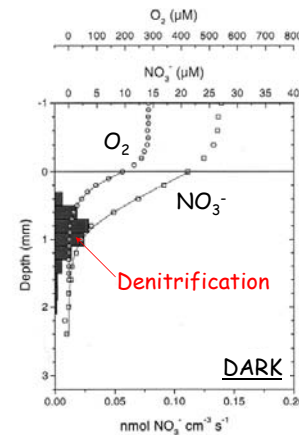
Kühl & Jørgensen 1992

Sulfur cycling in acidic lake sediment



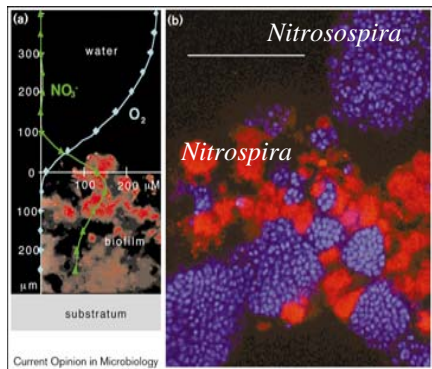
Kühl et al. 1998

Nitrogen cycling in diatom sediment



Combination of Microsensor Analysis and FISH in nitrifying biofilm

Nitrobacter



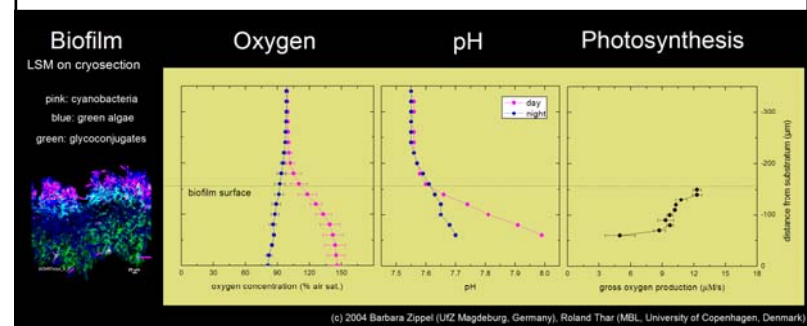
Examples of fluorescence *in situ* hybridization techniques.

- (a) *In situ* hybridization combined with microsensor measurements. *In situ* hybridization of a vertical biofilm slice with a carboxytetramethylrhodamine-labeled probe (NIT3) specific for the genus *Nitrobacter* (red stain cluster) correlated to oxygen and nitrate gradients measured by microelectrodes. Magnification, $\times 400$. Adapted from Schramm *et al.* [63].
- (b) Confocal microscopic image of a bacterial aggregate thin section after simultaneous hybridization with a Cy3-labeled probe specific for nitrite-oxidizing *Nitrosospira* sp. (red) and a Cy5-labeled probe specific for ammonia-oxidizing *Nitrosospira* sp. (blue). Scale bar indicates 20 μm (A Schramm, M Wagner, unpublished data).



Amann&Kühl 1998

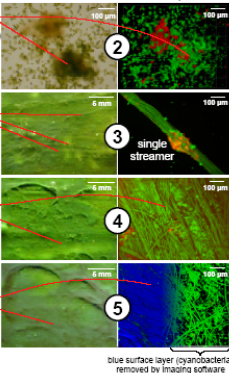
Combination of Microsensor Analysis and CLSM



(c) 2004 Barbara Zippel (UFZ Magdeburg, Germany), Roland Thar (MBL, University of Copenhagen, Denmark)

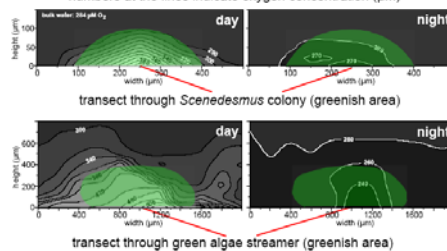
Light & Stereo Microscopy

biofilm surface shown in topview



2-dimensional oxygen distribution across biofilm microstructures

numbers at the lines indicate oxygen concentration (μM)



Thar & Kühl, in prep.

Microsensors

Advantages:

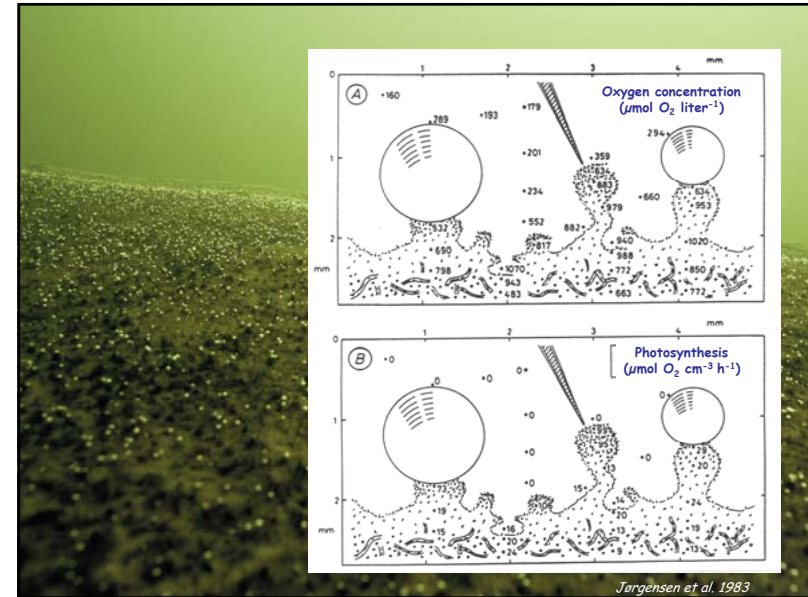
- ☺ Miniature instruments with electrochemical or optical detection principle
- ☺ 1-100 times thinner than a hair (0.001-0.1 mm tip diameter)
- ☺ Fast and specific response to analyte ($t_{90} < 0.2-60$ s)
- ☺ Commercially available

Disadvantages:

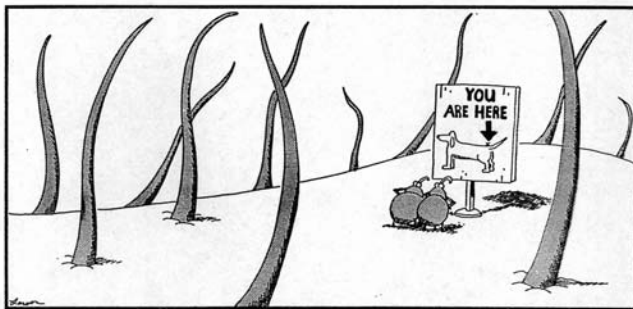
- ☹ Fragile and time consuming to prepare
- ☹ **NOT** non-invasive!!!!
- ☹ Point measurements

Microenvironmental Analysis of Biofilms

Part II - Imaging



Interfaces and Microenvironments



Spatial and Temporal Heterogeneity

Optodes for 2D O_2 mapping

Planar optodes
 Luminescent oxygen indicator
 immobilised
 in a hydrophobic matrix
 on a transparent carrier



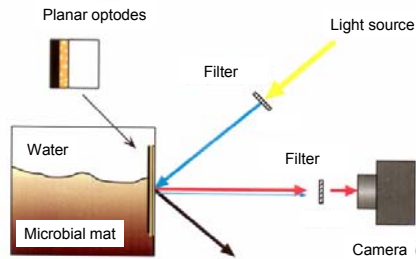
Fluorescence intensity imaging:

- need for O_2 permeable optical insulation
- non-transparent sensor foils

Fluorescence life-time imaging:

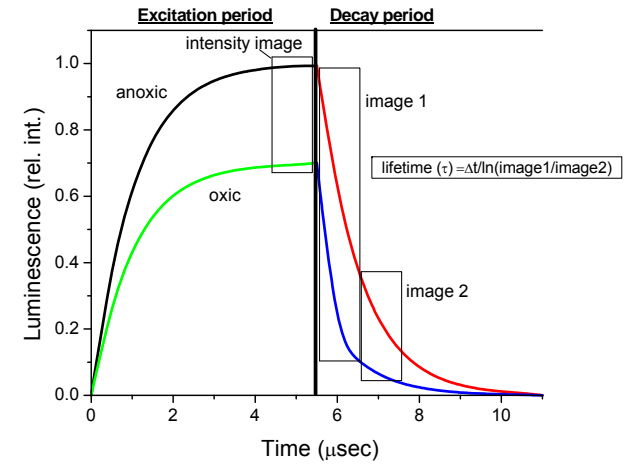
- transparent/semi-transparent sensor foils

Oxygen imaging



Glud et al. 1999

O₂ imaging: Intensity or life time based



Holst, Kohls, Klimant, König, Richter, & Kühl (1998)

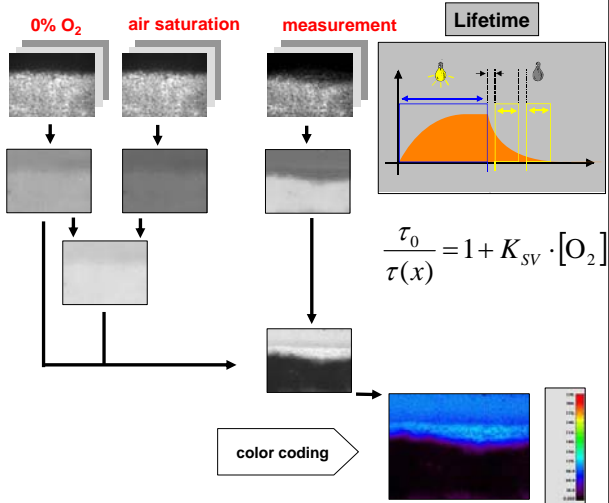
Image Processing

sets of 3 files are recorded:
•parameter file
•image window 1
•image window 2

conversion into lifetime image

calculation of K_{sv} image

conversion into O₂ image

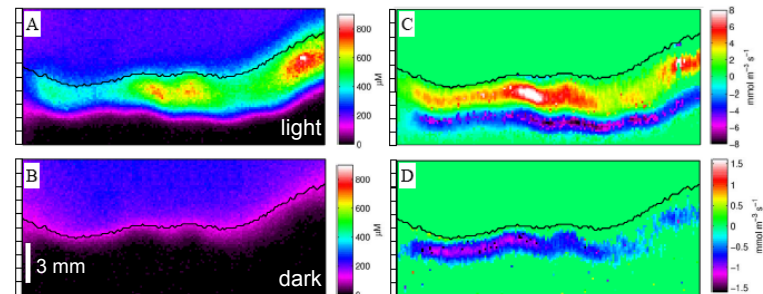


Holst et al. 1998, 2001

Oxygen and photosynthesis in a microbial mat

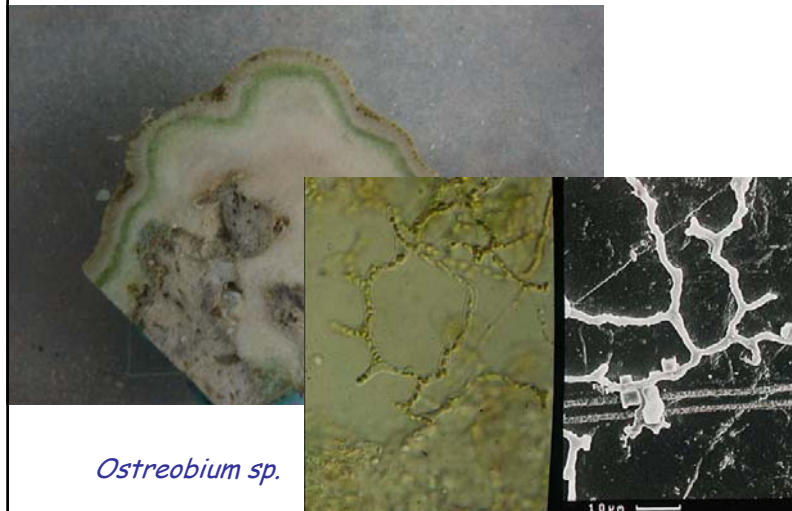
O₂ concentration

Photosynthesis & respiration

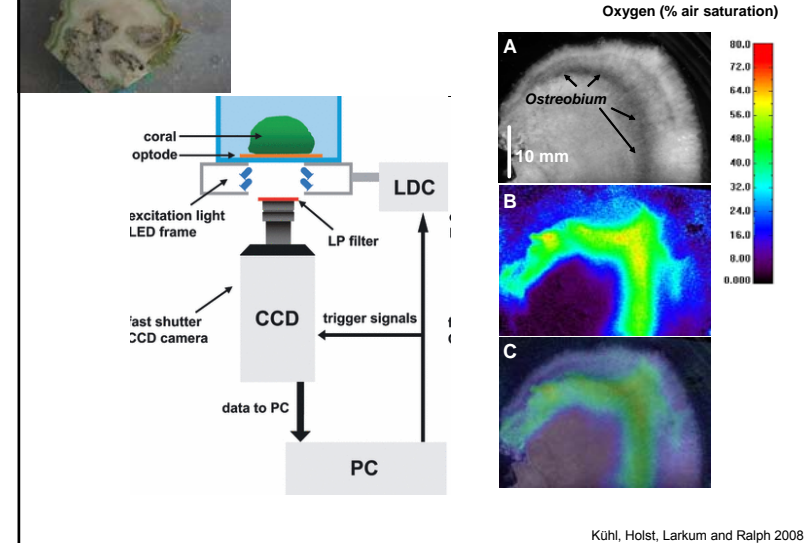


Kühl & Polerecky 2008

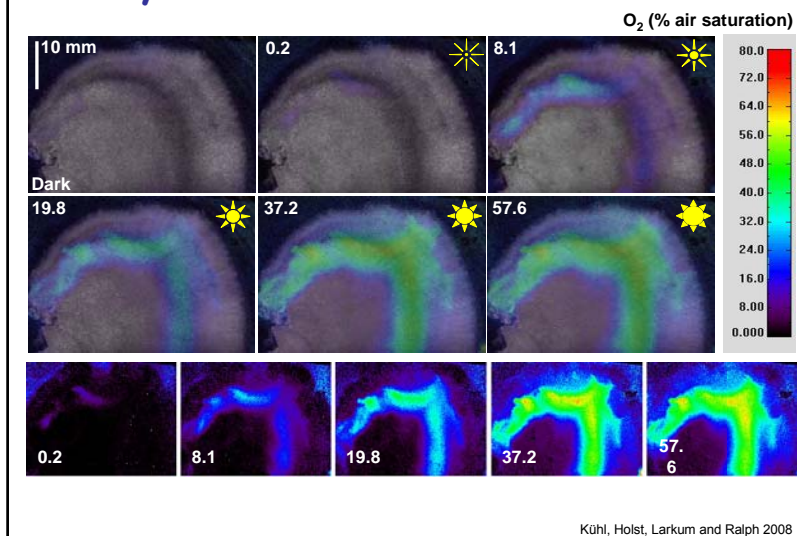
Endoliths in coral skeleton



Endolithic biofilm in corals

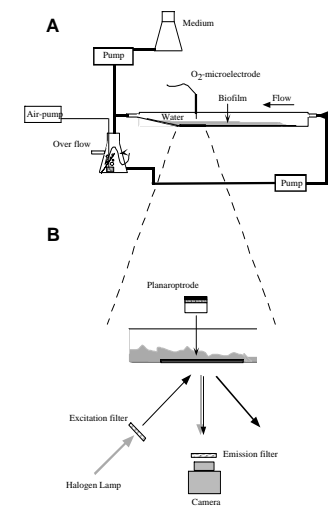


Photosynthesis in endolithic biofilms



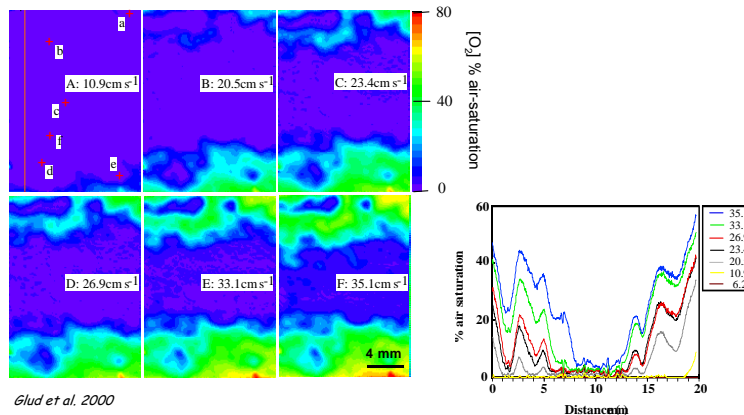
Biofilm reactor

Heterotrophic biofilm growing in complex organic medium on top of a planar oxygen optode.



Glud et al. 2000

Effect of flow on O₂ distribution at the basis of the biofilm

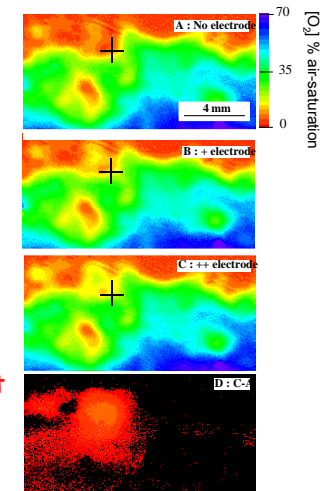


Glud et al. 2000

Effect of microsensor on O₂ distribution within biofilm

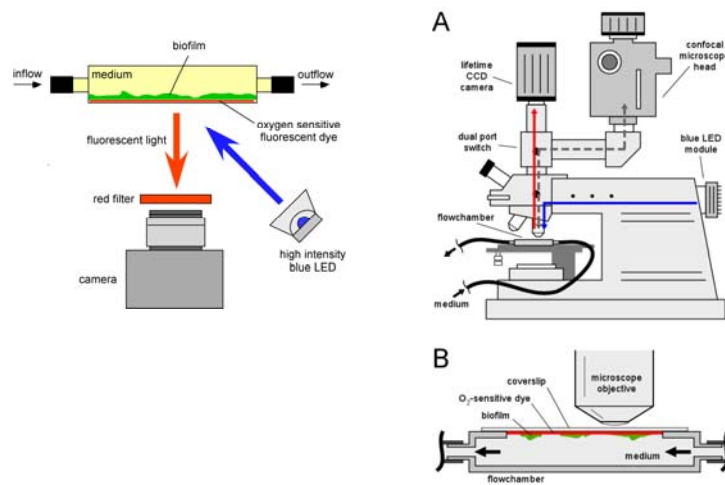
A microsensor was inserted in the biofilm at the cross.

The presence of the tiny microsensor tip disturbed the local oxygen microenvironment within the biofilm.

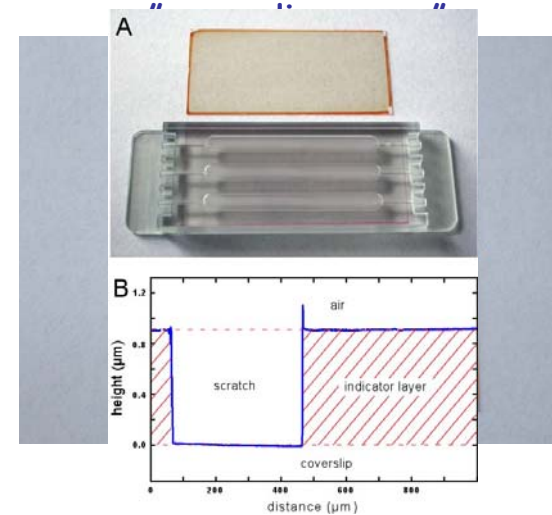


Glud et al. 2000

Flexible use with growth chambers



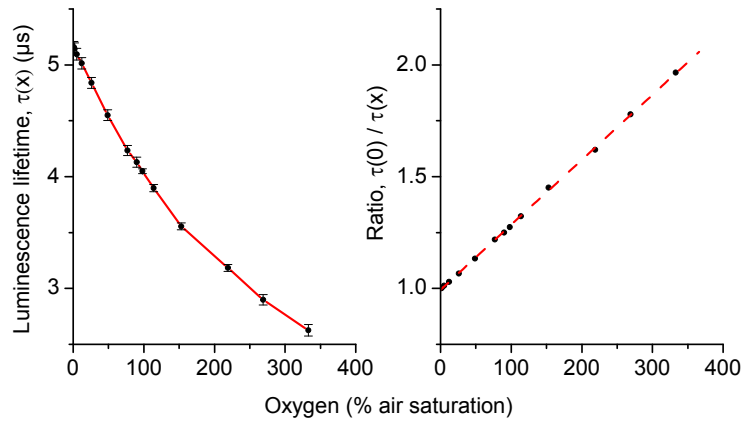
Planar oxygen nano-optode



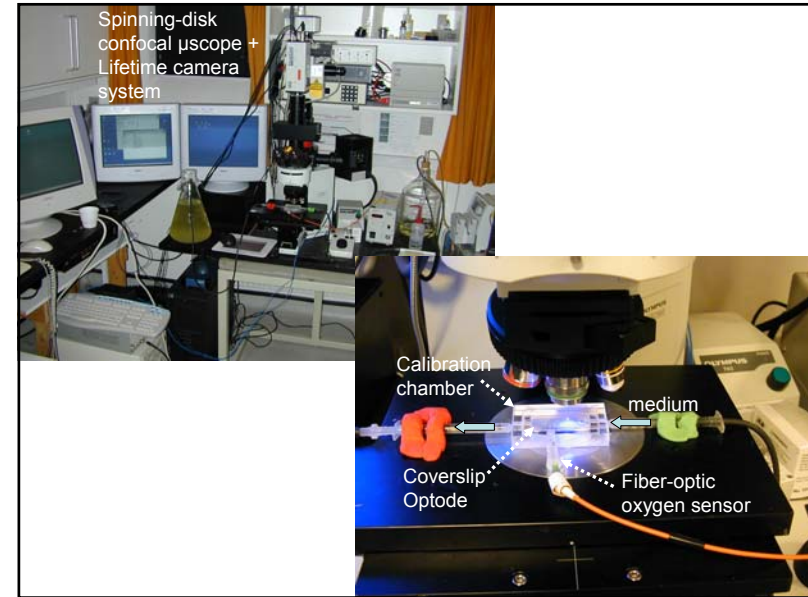
Kühl et al. 2007

Ideal Stern-Volmer quenching response

$$\frac{\tau_0}{\tau(x)} = 1 + K_{SV} \cdot [O_2]$$



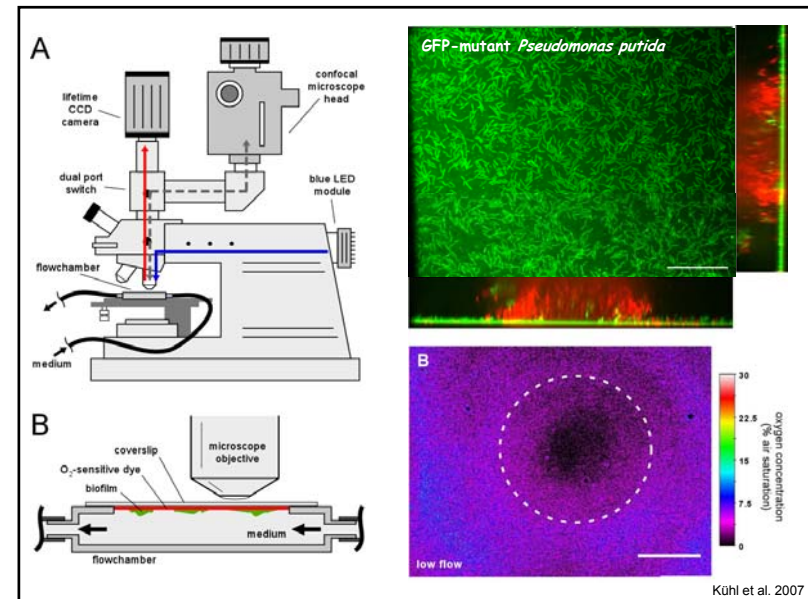
Kühl et al. 2007



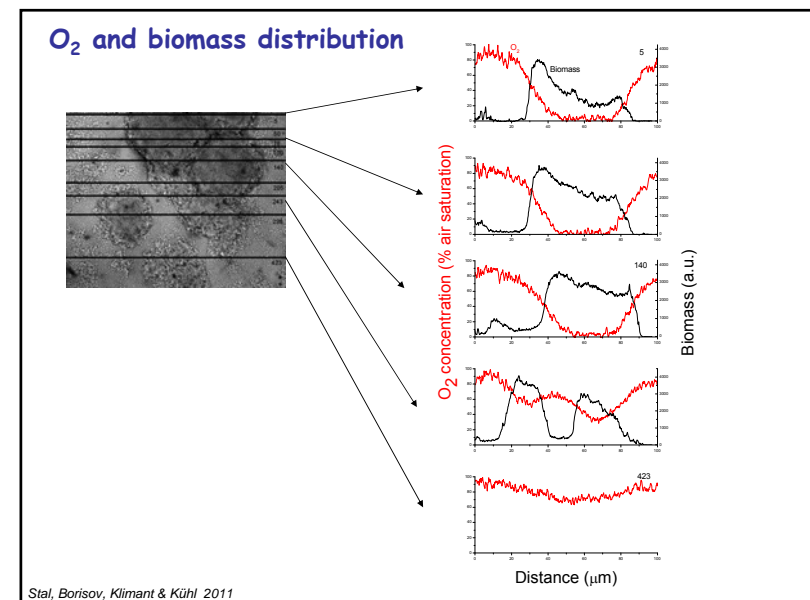
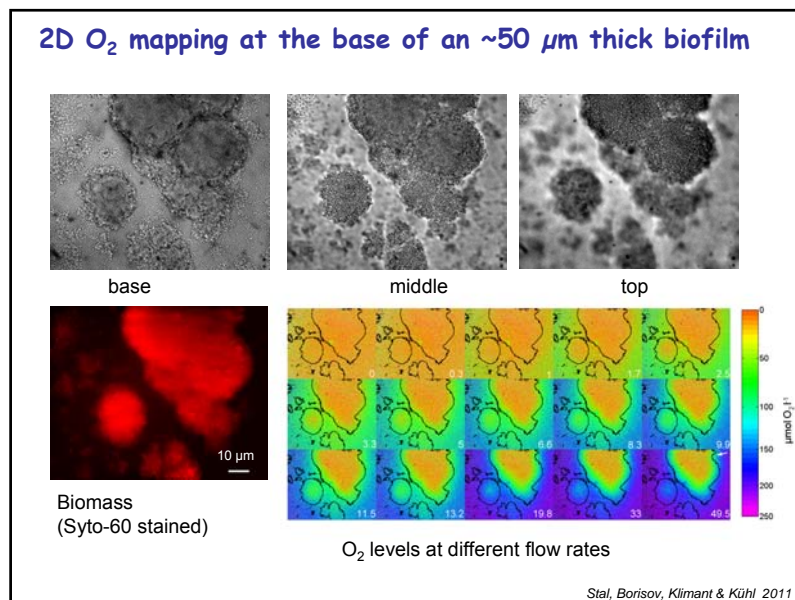
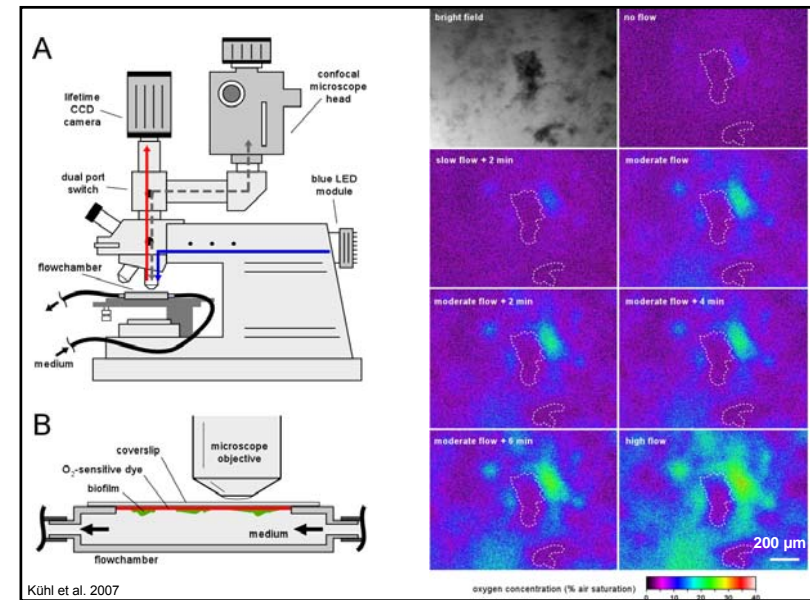
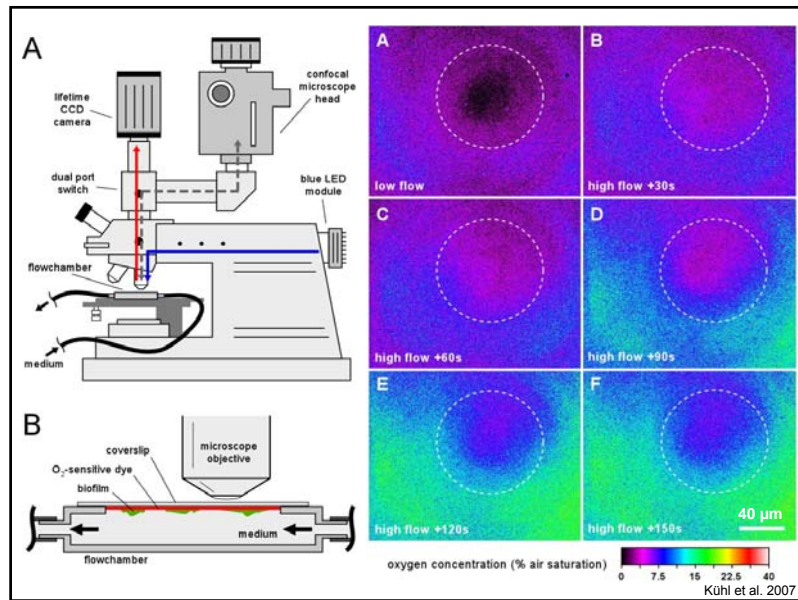
Flow-chamber biofilms growing on sensor



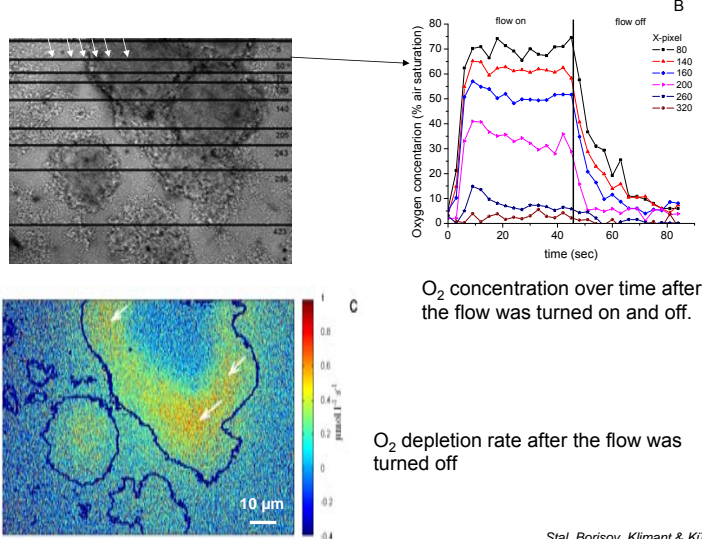
Kühl et al. 2007



Kühl et al. 2007



2D mapping of O₂ consumption

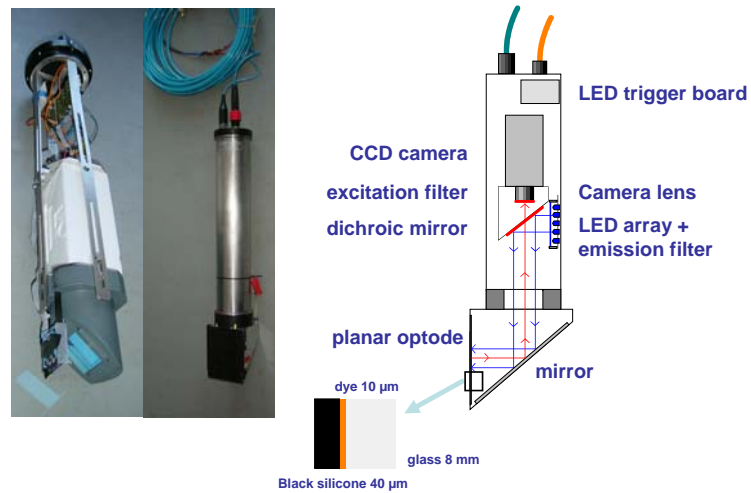


Stal, Borisov, Klimant & Kühl 2011

Microscopic O₂ imaging with planar nano-optodes

- Excellent tool for monitoring cell activity and biofilm growth on materials/surfaces.
- Combined imaging of chemical microenvironment, biofilm structure and GFP-expression in cells.
- Also useful for cell culture and tissue studies (e.g. test of biocides/antibiotics), materials science (e.g. biofouling prevention), and studies of many other surface-associated biological systems.

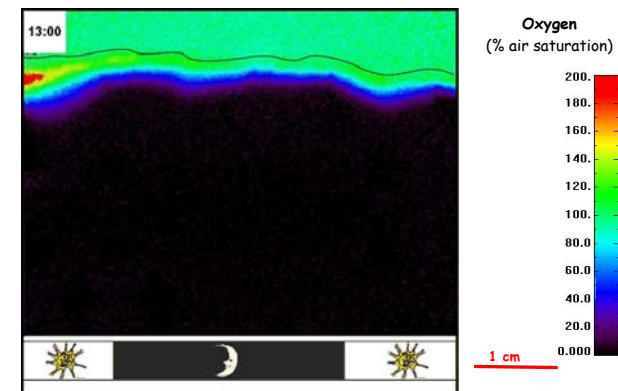
In situ planar optode module



Glud et al. (2001)

In situ oxygen dynamics

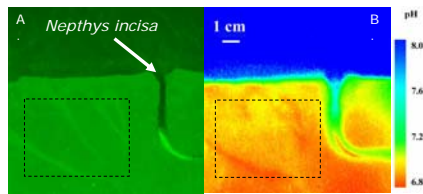
>24 hours time series in bioturbated sediment with microalgal biofilm 13:00 - 13:00; 1 image every 15 min)



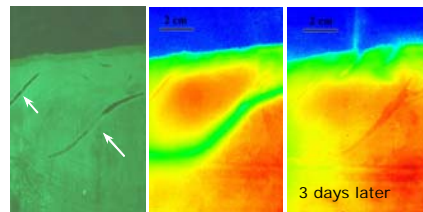
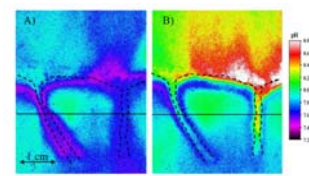
Wenzhöfer & Glud (2004)

Planar sensors for other biogeochemical solutes

Zhu et al 2006 Environ Sci Tech 39:8906-11
Zhu et al 2006 GeoChim Cosmochi 19:4933-49



Stahl et al 2006 L&O Meth 4:336-45



Zhu et al 2006 Mar Chem 101:40-53

NH_4^+ , H_2S , O_2 , pH, Enzymes, DGT/DET, SPI

Stromberg & Hulth 2005 Anal Chm 1-2:61-8
Robertson et al 2008 L&O Meth 6:502-512

Davison et al 1997 Nature 352:885-88
Davison et al 2000 IUPAC

Rhoads & Germano 1982 MEPS 25:253-94
Solán & Kennedy R 2002 MEPS 228:179-91

Rogers & Apté 2004 Environ Sci Tech 38:5134-40

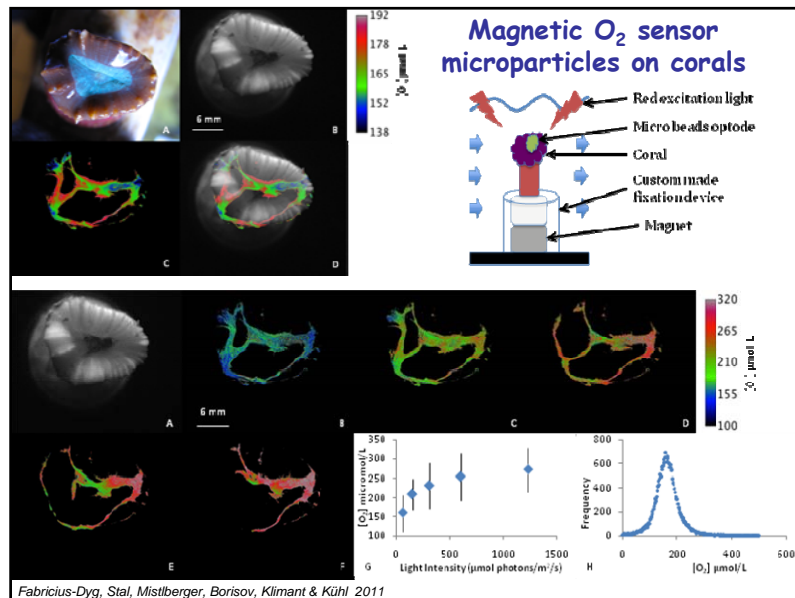
Planar optodes

Advantages:

- ☺ Miniature instrument array, i.e. a sensor foil, with optical detection principle
- ☺ 2D- mapping of analyte with (1-)50-100 μm resolution over several (μm^2) cm^2
- ☺ Relative fast and reversible response ($t_{90} < 1-30 \text{ s}$)

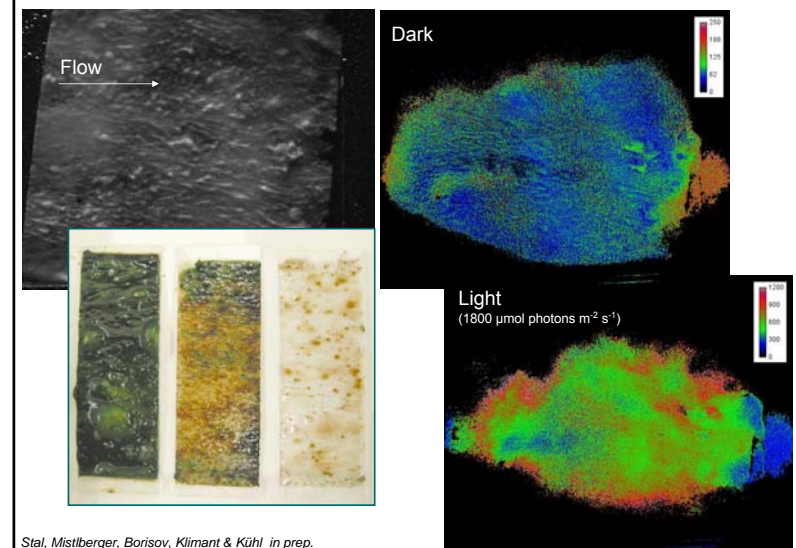
Disadvantages:

- ☹ Needs expensive imaging system and sophisticated software.
- ☹ **NOT** non-invasive!!!!
- ☹ Measurements at an "edge"
- ☹ Currently limited to O_2 , pH, NH_4^+ , CO_2 and temperature mapping in environmental applications



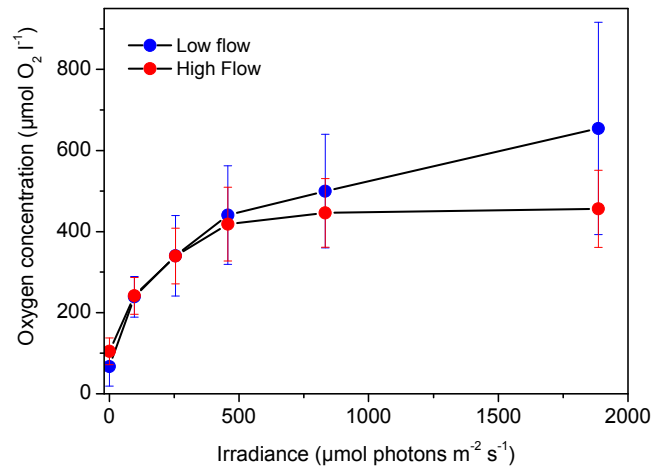
Fabricius-Dygg, Stal, Mistlberger, Borisov, Klimant & Kühl 2011

2D mapping of O_2 at the surface of biofilms



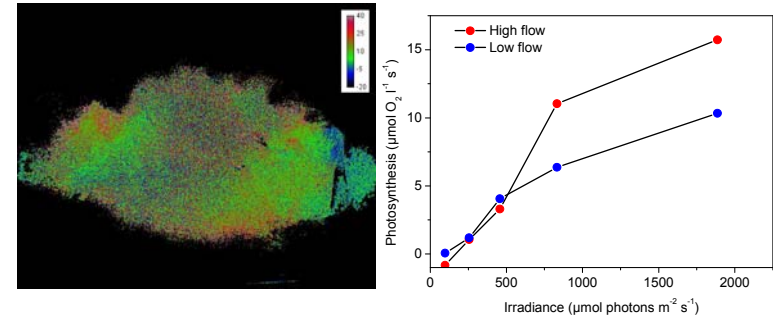
Stal, Mistlberger, Borisov, Klimant & Kühl in prep.

Mapping of O_2 vs. irradiance over the surface of a cyanobacterial biofilm



Stal, Mistlberger, Borisov, Klimant & Kühl in prep.

Mapping of gross photosynthesis over the surface of a cyanobacterial biofilm



O_2 depletion rate over first 2 seconds after darkening is taken as a proxy for gross photosynthesis

Stal, Mistlberger, Borisov, Klimant & Kühl in prep.